https://doi.org/10.1070/RCR5030

Variable-resistance materials for lithium-ion batteries

Evgenii V. Beletskii, Elena V. Alekseeva, Oleg V. Levin*

Institute of Chemistry, Saint Petersburg State University, Universitetsky prosp. 26, 198504 Peterhof, St. Petersburg, Russian Federation

The review focuses on variable-conductivity materials used to protect lithium-ion batteries from ignition. Examples of emergency situations arising in the operation of such batteries are given and their causes are considered. Thermal runaway that results in ignition of a lithium-ion battery and the chemical reactions accompanying this process are discussed. Internal battery protection using variable-resistance temperature- or voltage-sensitive components is described. Various approaches to the prevention of thermal runaway by modifying a battery with thermo- and voltage-resistive materials are summarized and analyzed. The advantages and drawbacks of various types of materials of this kind are demonstrated. Particular attention is paid to the practical significance of the creation and application of protective variable-resistance materials and approaches to the design of this kind of materials.
The bibliography includes 165 references.

Contents

1. Introduction 1
2. Types of critical processes and mechanism of thermal runaway 2
3. Use of thermoresistive materials for preventing thermal runaway 4
   3.1. Thermoresistive materials for controlling ionic conductivity 4
      3.1.1. Separators 4
      3.1.2. Electrolytes 4
   3.2. Thermoresistive materials for controlling electronic conductivity 4
      3.2.1. Operation principles of thermoresistive materials for preventing thermal runaway 4
      3.2.2. Composites of crystalline polymers with electrically conductive fillers 6
      3.2.3. Conductive polymers 7
      3.2.4. Thermoresistive conductive additives to the cathode material 8
      3.2.5. Application of variable-resistance materials in negative electrodes 9
4. Use of potentioresistive materials to prevent thermal runaway 10
   4.1. Principles of operation of potentioresistive materials 10
   4.2. Potentioresistive materials for controlling electronic conductivity 10
      4.2.1. Separators 10
      4.2.2. Positive electrode 11
5. Conclusion 13
6. List of abbreviations and symbols 14
7. References 14

1. Introduction

Over the past three decades, lithium-ion batteries (LIB) have been increasingly used as the main power sources in portable electronic devices, in stationary energy storage systems and in the transport.[1,2] Manufacturers of such devices claim that batteries are safe, but the use of active oxidants and reducing agents along with organic electrolytes carries the risks of ignition and explosion that may cause destruction and injuries whose severity ranges from minor superficial burns to death. According to the US National Fire Incident Reporting System (NFIRS), 1013 fires caused by ignition of LIB in various devices have been reported in the period from 1999 to 2013. The US Consumer Product Safety Commission (USCPSC) reported 25 000 similar cases in the subsequent five-year period, up to February 2018.[3]

As a rule, ignition results from the so-called thermal runaway, *i.e.*, an abrupt temperature increase due to internal or external overheating associated with abnormal battery operation conditions. Therefore, it appears particularly important to develop mechanisms that prevent thermal runaway. A number of protective strategies exist that are aimed at creating external protective systems and at modifying an electrolyte and electrodes using functional materials. Traditionally, the battery design involves electronic monitoring and control systems as external protection. They comprise sensors, actuators such as connectors (breakers), controllers linked by numerous connections and wired to a processor that handles the incoming signals

E.V.Beletskii. Junior Researcher, Department of Electrochemistry, Institute of Chemistry, SbSU.
E-mail: st803431@spbu.ru
Research interests: conductive polymers, protection of lithium-ion batteries from overcharge, overdischarge, and short circuit; plasma electrochemistry.
E.V.Alekseeva. Candidate of Chemical Sciences, Senior Researcher at the same Department.
E-mail: alekseeva_ev@yahoo.com
Research interests: conductive polymers, low-temperature batteries, polymer complexes of transition metals with Schiff bases.
O.V.Levin. Doctor of Chemical Sciences, Professor at the same Department.
E-mail: o.levin@spbu.ru
Research interests: conductive polymers, batteries, photoelectrochemistry, fuel cells.

Translation: S.S.Veselyi

Received 22 June 2021

© 2022 Uspekhi Khimii, ZIOC RAS, Russian Academy of Sciences and IOP Publishing Limited

by a dedicated algorithm.[4] These systems are complemented by mechanical circuit breakers and fuses.

More reliable approaches include chemical protection elements that duplicate or supplement the functions of electronic monitoring and control systems. The most common elements used for this purpose include functional additives to an electrolyte, such as additives that slow down the formation of lithium dendrites;[5–7] redox shuttle additives that prevent overcharging by electrochemical shunting;[8–11] irreversible overcharge interrupters acting directly to generate a signal for an external device that should disconnect the battery from the charging circuit (for example, due to abundant gas formation);[12,13] fireproofing additives,[14–16] and the use of totally non-combustible electrolytes.[17–24]

A common drawback of these additives is that they can suppress only one specific stage involved in the development of an emergency situation. In this case, many protective mechanisms are only activated after the beginning of an irreversible process of battery failure and can only minimize the accident consequences. Moreover, changing the electrolyte composition affects all the components of batteries, so apart from the protective properties, it has to be ensured that each new additive is devoid of side effects. Therefore, chemical protective systems that do not require the electrolyte composition to be modified and can operate reversibly are being actively searched for. The most common systems of this kind include fusible separators that interrupt the electrical circuit if the temperature rises to the melting point due to a sharp decrease in the number of available pores for the transport of lithium ions[25] and variable-resistance materials contained in the electrodes, which interrupt the electronic conductivity chain if the temperature increases or if the battery voltage goes beyond the allowed limits. Internal protection by means of thermo- and potentio-resistive layers is one of the versatile solutions to the LIB safety problem since it allows all undesirable processes associated with an increase in the temperature or voltage (overcharge, overdischarge, external and internal short circuit, overheating) to be interrupted at their initial stage, whereas all the other methods usually aim at protection against some single process, mainly overcharge or overheating.

At present, there are no specialized review articles dealing with variable-resistance materials, while general reviews (see, for example, Refs 26–28) each devote a single paragraph to such materials, where compositions are listed and some electrochemical results are given. Therefore, it became necessary to publish this thematic review summarizing the array of literature data on variable-conductivity materials.

2. Types of critical processes and mechanism of thermal runaway

Thermal runaway is the main cause of ignition and explosion of LIB.[29] It occurs due to a sharp increase in temperature inside a battery for a short time, which results in decomposition of the reactive materials of the positively and negatively charged electrodes and ignition of the electrolyte.[30] Various critical situations are known that can cause the thermal runaway during LIB operation,[31–33] for example:

— overcharge, *i.e.* feeding a battery with an amount of electricity above the nominal value;[34–36]

— overdischarge, *i.e.* a phenomenon that occurs when the battery is discharged below the safe voltage limit determined by the nature of the electrodes;[37,38]

— external and internal short circuit, *i.e.* connecting the positive and negative electrodes by an electron conductor that results in a high local current density and produces strong heating;[39–41]

— overheating, *i.e.* a temperature rise to a threshold value where battery components start to decompose and react with one another with heat evolution;[42]

— mechanical damage to the battery.[43]

Overcharge results in heat release[34,44] and growth of lithium dendrites as the intercalation capacity of the negative electrode is exceeded. If the temperature does not reach the values where thermal runaway develops, the growth of lithium dendrites through the separator causes internal short circuit followed by intense heat release.[45–47] A similar process occurs in the case of overdischarge.[37,48] The destruction of the solid electrolyte interface (SEI) and the growth of copper dendrites through the separator, as well as external or internal short circuit due to other reasons, cause intense heat generation[32,49,50] that can be yet another reason of thermal runaway.[39,51]

The likelihood of the beginning of thermal runaway is determined by the LIB temperature, which depends on the balance between the amount of released and dissipated heat.[52–54] Heat release exponentially depends and dissipation linearly depends on the duration of the critical process.[55,56] As the battery is heated above a certain temperature that varies from 80 to 150 °C depending on the composition of the cathode material,[42,57] exothermic chemical reactions between the electrodes and the electrolyte begin. If the battery can dissipate heat generated in these reactions, the temperature will not rise above the critical value. However, if the amount of heat released is greater than the dissipated amount, then exothermic processes occur under nearly adiabatic conditions, which entails a sharp increase in temperature, a further acceleration of chemical reactions and release of an even greater amount of heat, which is a beginning of thermal runaway.[58,59]

The thermal runaway causing the destruction of a LIB occurs in three stages (Fig. 1):[42]

— heating start,

— heat accumulation,

— ignition and explosion.

Each stage corresponds to certain processes.[29,42,50,57,60,61] At the first stage, the temperature of the battery begins to rise. The reasons for the onset of overheating may vary, including defects during the manufacture of the battery or its mechanical damage,[62,63] wrong

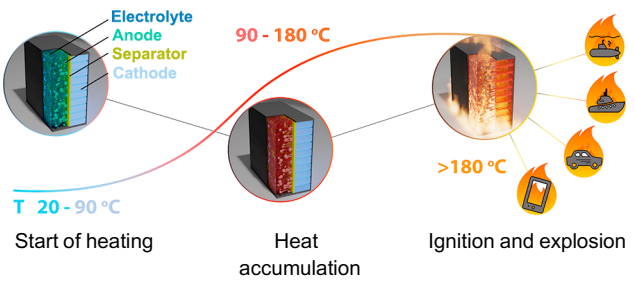


Figure 1. Three stages of thermal runaway. The drawing was created by the authors based on data from Ref. 42.

temperature mode of operation,[64–66] overcharge or over-discharge,[44, 48, 67, 68] formation of dendrites[69–72] due to fast charging modes or charging at low temperatures, *etc*. A small zone or a few local zones that heat up more strongly than others appear, and the second stage of thermal runaway begins in those zones.[50]

The second stage, *i.e*. the stage of heat accumulation following the initial heating, may be accompanied by a number of phenomena, such as SEI destruction,[62, 73] a reaction of the anode material with electrolyte components, meltdown of the separator, and interaction of the cathode material with the anode material and with electrolyte components.[29, 50] Each of these processes increases the heating rate. The SEI layer consists of stable components (*e.g*. LiF and Li_2CO_3) and metastable ones (such as polymers, $ROCO_2Li$, $(CH_2OCO_2Li)_2$ and ROLi).[62, 74] Metastable components can decompose exothermically at >90 °C with evolution of flammable gases and oxygen. The decomposition of the SEI is the first exothermic reaction with a heat of 257 J g^{-1} with respect to carbon,[62] which initiates thermal runaway,

$$(CH_2OCO_2Li)_2 \longrightarrow Li_2CO_3 + C_2H_4 + CO_2 + 0.5\,O_2 \quad (1)$$

$$2\,LiC_6 + (CH_2OCO_2Li)_2 \longrightarrow 2\,Li_2CO_3 + C_2H_4 + 12\,C \quad (2)$$

As a result, the temperature inside the battery increases. On exposed areas of the negatively charged electrode, metallic or intercalated lithium reacts with organic solvents such as ethylene carbonate (EC), diethyl carbonate (DEC), dimethyl carbonate (DMC) or propylene carbonate (PC) to release flammable hydrocarbons and various reactive products in accordance with the following general scheme for various electrolytes: [29, 62, 75, 76]

$$LiC_6 + \text{solvent} \longrightarrow Li_2CO_3 + C_2H_4 + C + \quad (2a)$$
$$+ C_2H_6 + C_3H_6 + ROLi + ROCO_2Li + Li_2C_2O_4 +$$
$$+ \text{esters and ethers} + \text{alcohols}$$

where the solvent is $C_3H_4O_3$, $C_5H_{10}O_3$, $C_3H_6O_3$ or $C_4H_6O_3$.

The reaction products of the anode material and electrolyte are the main components of the SEI, so the reaction could be called 'SEI regeneration reaction'.[74, 77] However, the solid electrolyte interface cannot efficiently protect metallic lithium formed on the surface of the negative electrode from further reactions with the electrolyte. Hence, the undesirable process on the negative electrode will continue.

At $\geqslant 130$ °C, the separators, *i.e*. the polymeric structures arranged between the battery electrodes and typically made of a few layers of polyethylene (PE) and polypropylene (PP), begin to melt,[78] which favours the further process and causes a large-scale short circuit between the positive and negative electrodes. The use of multilayer separators in which a layer of lower-melting polyethylene is arranged between polypropylene layers partially prevents further thermal runaway due to an increase in internal resistance to ion transport and blocking of high currents in the case of overcharging and sometimes in the case of short circuit.[79, 80] However, in the case of overheating, exothermic reactions may be due to reasons other than the passage of current; in such a case, an increase in the separator resistance blocks the thermal runaway to a limited extent. With a further increase in temperature, the separator shrinks and ceases to perform its functions.[81] Its shrinkage can result in a local contact of positively and negatively charged electrodes, *i.e*. short circuit, which would produce a significant amount of heat and promote further separator destruction.[58]

The released heat causes the cathode material to decompose and results in oxygen release in the case of materials based on mixed oxides.[82–84] The decomposition temperature depends on the type of the material.[85] The first example is $LiCoO_2$, one of the main high-voltage cathode materials, which decomposes at a temperature of >180 °C (see Ref. 29)

$$Li_xCoO_2 \longrightarrow \quad (3)$$
$$\longrightarrow x\,LiCoO_2 + 1/3\,(1-x)\,Co_3O_4 + 1/3\,(1-x)\,O_2$$

$$Co_3O_4 \longrightarrow 3\,CoO + 0.5\,O_2 \quad (4)$$

$$CoO \longrightarrow Co + 0.5\,O_2 \quad (5)$$

The second example is the mixed oxide $LiNi_xMn_yCo_zO_2$ ($x:y:z = 4:3:3$), which in partially charged state decomposes at a temperature of >280 °C (see Ref. 86)

$$Li_{0.34}(M^{3.66+})_{1.0}O_2 \longrightarrow \quad (6)$$
$$\longrightarrow \frac{67}{150}\left(Li_{51/67}(M^{3.23+})_{150/67}O_4\right) + \frac{8}{75}O_2\uparrow$$

where $M = Ni_xMn_yCo_z$.

All the reactions presented above are also exothermic. The heat accumulation stage lasts until a sufficient amount of oxygen and combustible gases have accumulated to start ignition, which is the third and final stage of thermal runaway.[29, 32]

Once the thermal runaway mechanism discussed in detail in a number of reviews[57, 87–89] is understood, it becomes possible to develop various approaches to reduce the risk of ignition and explosion by rational design of batteries and by creation of safe materials. Based on literature sources dealing with the problem of ensuring the safe operation of batteries,[42, 43, 59, 72, 90–92] we can single out such a promising and dynamically developing approach as the creation of protective thermo- and potentio-resistive formulations comprising materials whose electrical resistance abruptly changes as a threshold temperature or voltage is exceeded. Such layers are arranged inside a battery, and as a result, its internal resistance increases in an emergency situation.

If charging (or discharging) occurs in galvanostatic mode and the current is maintained by a galvanostat, then an increase in resistance would lead to an even more intense release of Joule heat calculated as the square of current multiplied by the battery resistance and by the time of its operation. However, the operation of LIB usually occurs in more complex modes that differ from the operation of single cells and batteries. In particular, the typical mode in which a single battery is charged involves charging with a constant current to a constant voltage using a low-power charging unit. If safety circuits fail, the charging unit can supply arbitrary current and voltage to the battery, but their product would be limited by the power of the device. The cell voltage increases, but due to the increase in the protective layer resistance, the supplied current decreases significantly, which in turn results in a decrease in heat generation. If a cell operates as part of a battery, then variable-resistance protective layers can also serve as a source of the control signal for the monitoring and control system. A sharp increase in the voltage of a damaged cell

caused by an increase in the resistance of the protective layer is easily detected by electronic circuits and thus serves as a signal for the emergency shutdown of the battery. If the protective layer is activated by a short circuit, the heat released upon full discharge is determined only by the cell capacity and voltage. However, a discharge with increased layer resistance takes a longer time than in the case of short-circuiting of an unprotected battery's contacts, so the released heat has time to dissipate and does not cause thermal runaway.

Thus, variable-resistance materials play an important role in the LIB protection. However, it should be noted once again that variable-resistance materials receive insufficient attention in the well-known reviews dealing with the problems of battery safety.

3. Use of thermoresistive materials for preventing thermal runaway

3.1. Thermoresistive materials for controlling ionic conductivity

3.1.1. Separators

One of the well-known approaches for preventing thermal runaway involves the use of thermoresistive materials whose ionic conductivity can decrease with an increase in temperature. Typical examples of such materials include porous polymer structures, for example, a three-layer separator that has become an integral part of all commercial LIBs. An increase in temperature causes the components of these materials to melt and 'seal' the pores. Systems or this kind were sufficiently described in a number of review articles[25,93–95] and are mentioned here only for completeness of the discussion, so we present just a few most representative examples.

Zhang *et al.*[79] report a temperature-sensitive separator obtained by applying a thin layer of polyethylene microspheres onto a commercial porous polypropylene membrane. The results of structural and thermal analysis showed that the coating had a porous structure that allowed charge–discharge to occur at room temperature. If the temperature increases to 110 °C, the membrane material melts and ion transport stops within 3 s, or within 1 s at 120 °C.

The possibility of using a polypropylene separator coated with silicon dioxide nanoparticles, which are encapsulated in a polystyrene–poly(butyl acrylate) copolymer, as a 'thermal switch' was considered.[96] The melting temperature of the composite separator was 80 °C. The polymer of the shell can slow down the diffusion of lithium ions in the polypropylene separator at the glass transition temperature, thereby increasing its resistance and preventing the thermal runaway of the battery, while the silicon core nanoparticles protect the separator from significant thermal shrinkage if the temperature continues to increase. Moreover, the electrochemical characteristics of such a separator do not degrade in normal operation. In perspective, the temperature of thermal shutdown can be further controlled by varying the volume ratio of polystyrene and poly(butyl acrylate).[97]

3.1.2. Electrolytes

There are two main ways to improve the safety of batteries by means of electrolytes:

— using various additives,

— using polymer electrolytes.

The most common methods of modifying the protective properties of the electrolyte include the use of additives that prevent the electrolyte ignition or additives that prevent the battery from overcharge. These methods are beyond the scope of this review. They are covered in specialized review articles (see, for example, Ref. 90).

As a rule, as the temperature increases, the conductivity of polymer electrolytes increases exponentially. Therefore, they cannot block ion transport at the beginning of thermal runaway. However, there are variable conductivity electrolytes that can slow down its increase under strong heating. For example, an electrolyte based on poly(ethylene oxide) (PEO) with lithium trifluoromethylsulfonate (triflate) embedded in an alumina nanoporous ceramic membrane can be used for protection against thermal runaway.[98] The electrical conductivity of this composite increases from 10^{-7} to 10^{-5} S cm^{-1} with an increase in temperature from 20 to 65 °C. The conductivity nearly does not increase any more. This behaviour is explained by the interaction of PEO polymer chains with aluminium oxide inside cylindrical pores, which results in a slowdown of the ion motion velocity.

Yet another variant of protection involves the transition of the electrolyte from a liquid state to a gel-like state upon heating, accompanied by an increase in resistance. It was proposed[99] to use poly(*N*-prop-2-ylacrylamide-co-acrylamide) for the thermal protection of supercapacitors with a response temperature of ~50 °C. It is known that an increase in temperature can result in the transition of this compound from hydrophilic to hydrophobic state. Thus, as the environment temperature increases, the copolymer forms a hydrogel due to hydrophobic association, thus inhibiting the migration of conductive ions between the electrodes. As the hydrogel cools down, the copolymer returns to its original state and the operation of the supercapacitor is restored.

3.2. Thermoresistive materials for controlling electronic conductivity

3.2.1. Operation principles of thermoresistive materials for preventing thermal runaway

Modification of battery electrodes is one of the most important ways to prevent thermal runaway.[31,59] The primary causes of thermal runaway may include both a temperature increase and the voltage going beyond the permissible range, so the creation of electrodes that can interrupt the current by increasing the internal resistance of the battery when the critical voltage and(or) temperature is reached is a task of current interest.[100,101] One of the main approaches to the solution of this problem involves the deposition of an intermediate thermal or potentio-resistive layer that separates the active mass of the electrode from the current lead,[102–106] or incorporation of thermo- or potentio-resistive current-conducting additives into the active mass of the electrode.[107,108] The mechanisms of action of the protective element shown in Fig. 2 do not depend on the method of electrode modification.

The resistance of the thermoresistive component can increase with an increase in temperature due to a positive temperature coefficient (PTC).[102] Two types of substances that have this property are known:

— composites of crystalline polymers with electrically conductive fillers,

— true conductive polymers.

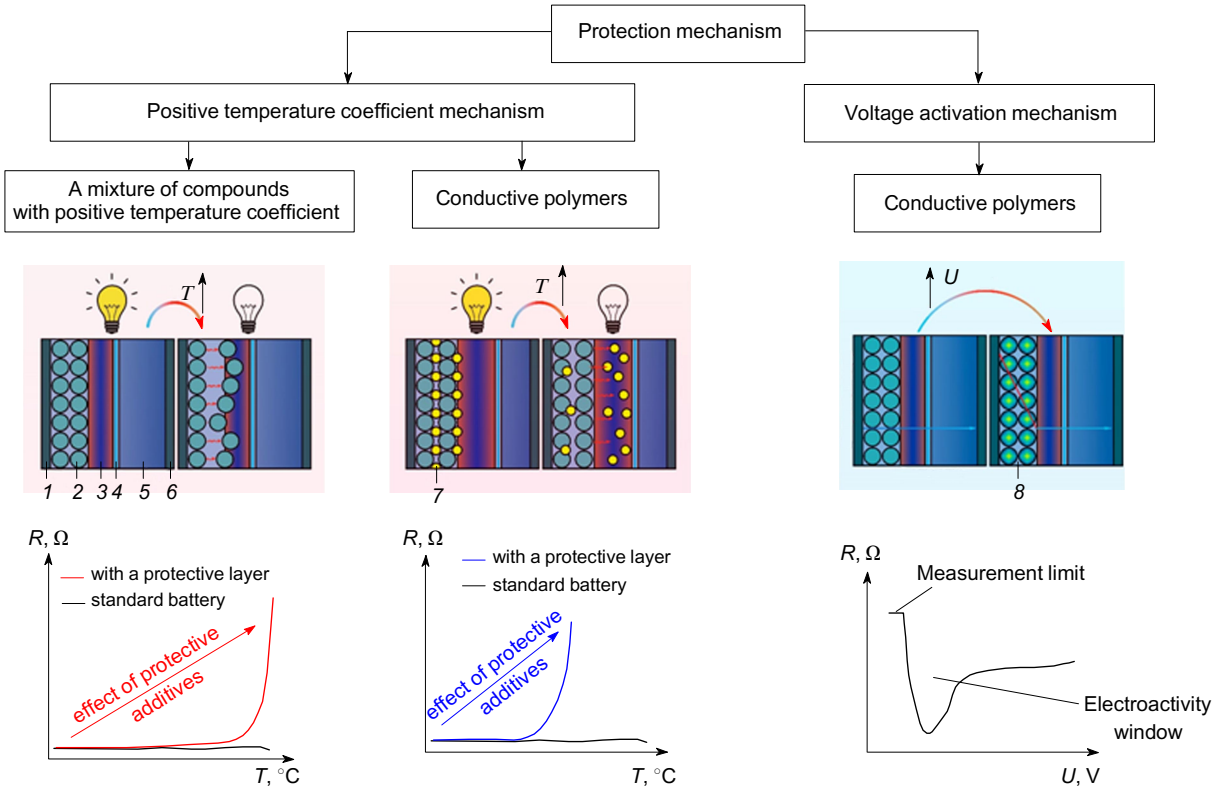


Figure 2. Mechanisms of operation of thermoresistive and potentioresistive protective elements. The drawing was created by the authors based on data from Refs 105, 108, 115. *R* is resistance, *U* is voltage, (*1*) aluminium current lead, (*2*) thermoresistive layer, (*3*) cathode mass, (*4*) separator, (*5*) anode mass, (*6*) copper current lead, (*7*) counter-ions in the structure of the electrically conductive polymer, (*8*) electrically conductive polymer.

In composite materials of the first type, the electrically conductive particles are distributed in a polymer matrix that does not conduct electric current, so ohmic contacts exist between the filler particles under normal conditions (see Fig. 2).[108] Long chains of such particles that contact each other provide the electrical conductivity of the material as a whole.

An increase in temperature affects the properties of composites in a complex way. Electrically conductive polymer composites can undergo significant changes in electrical resistance that may be characterized by either positive or negative temperature coefficients.[109, 110] At low temperatures (from −50 to 50 °C) where the contact between conductive particles is stable, an exponential decrease in electrical resistance with an increase in temperature characteristic of semiconductors is observed.[111–113] An increase in electrical resistance usually begins at higher temperatures, which is attributed to the thermal expansion of the polymer matrix and the loss of contact between the conductive particles.[114] Upon further increase in temperature, the polymer matrix melts, leading to an abrupt increase in electrical resistance.[114] The difference of this process from the expansion of a solid polymer matrix is that the increase in the polymer volume upon melting results not from its uniform expansion but from a combination of processes involving an enlargement of the melt microvolumes (the first drops formed upon melting of defective crystals) surrounded by crystallites. Eventually, destruction of electrically conductive paths in the intergranular zones occurs as micro-deformations and micro-stresses appear.[114]

In most cases, a combination of these processes results in a resistance increase by a factor of tens to millions on heating from room temperature to the melting point of polymers (100–200 °C).[114]

Electrically conductive polymers are yet another class of materials that demonstrate an increase in resistance upon heating.[102, 103, 115] Though the resistance–temperature plots are formally alike, the reasons of this effect in electrically conductive polymers and composite materials based on them differ.

Electrically conductive polymers contain long chains of conjugated π-bonds. The transition to the conductive state occurs by partial oxidation. As a result, mobile delocalized positively charged quasi-particles, or polarons, are formed in these conjugated chains. The charge of these quasi-particles is compensated by doping the polymer with counter-ions.[116] The stability of the doped state depends on the nature of the counter-ion, the temperature,[117, 118] and the nature of the environment[119, 120] and the polymer.[117, 121] The mechanism of the loss of electrical conductivity upon heating in electrically conductive polymers involves the destruction of polarons, which results in the release of counter-ions from the polymer matrix or to their decomposition followed by transition of the polymer to a neutral state (see Fig. 2).[107] Such a behaviour was observed in polythiophene (PT) and its derivatives,[107, 121, 122] polypyrrole[122] and the polymeric complex poly-[*N*,*N*′-ethylenebis(3-methoxysalicylideneiminato)nickel(II)]-(poly[Ni(MeOSalen)]).[116] After cooling of the latter polymer, the counterions are able to reenter the polymer matrix

with restoration of electrical conductivity upon electrochemical oxidation (reduction). Different thermoresistive materials used to modify electrodes are compared using such concepts as the transition temperature (T_c), *i.e.* the temperature where the resistance increases more than two-fold relative to the initial value,[106] and the response intensity (I_c), *i.e.* the ratio of the maximum resistance to the resistance at room temperature (T_r). The intensity logarithm is used sometimes.[123]

3.2.2. Composites of crystalline polymers with electrically conductive fillers

Composites of crystalline polymers with conductive fillers can be used to interrupt the electronic conduction circuit within a battery. Despite the fact that composites are based on various crystalline polymers and electrically conductive fillers, their effect on the electrochemical behaviour of the battery will be the same, as Fig. 3 shows schematically. At room temperature, the performance is not affected. In the above example, T_1 is the transition temperature where the composite resistance begins to increase. A resistance increase with temperature rise up to the temperature of the maximum transition intensity ($T_2 \geqslant T_m$, where T_m is the melting temperature) results in cell failure: the resistance increases significantly, while the discharge capacity decreases several-fold (see Fig. 3 *b*).

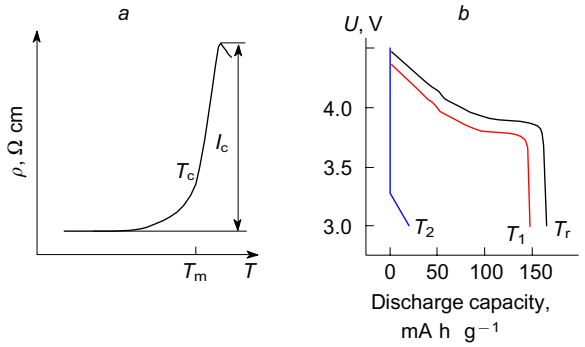


Figure 3. Schematic drawing of the temperature dependence of the resistance of low-molecular-weight polyethylene with carbon black (*a*) and the dependence of voltage on the discharge capacity for an LCO–PTC composite (additive)/Al electrode with a current of 0.1*C* at T_m, T_1 and T_2 (*b*). See the text for the I_c, T_c, T_m, T_r, T_1 and T_2 values; ρ is the resistivity. The drawing was created by the authors based on data from Refs 103, 124.

Poly(1,1-difluoroethylene) (PDFE),[106] epoxy resin (ER),[124] PE [125] and poly(methyl methacrylate) (PMMA) [126] are used as crystalline polymers, while carbon black, nickel and a nickel–graphene composite are used as conductive fillers. The characteristics of these composites are presented in Table 1. The transition temperature is close to 80 °C in all cases,[106] whereas the temperature of the maximum transition intensity depends on the composition of the composite. In the case of PMMA and ER, it equals 140 °C,[124, 126] for PEO with poly(ethylene-co-vinyl acetate) (EVA) it is ~100 °C,[125] and in the case of PE with spiky nickel oxide, it is 80 °C.[108] The data presented above indicate that the transition of the composites from the conductive to the insulating state occurs in a narrow temperature range. The transition intensities of these materials vary greatly: the resistance changes by a factor from tens to hundreds. The PE composite with spiky nickel oxide stands out in this respect, demonstrating a 10 000-fold increase in resistance upon heating; thus it can be considered as an insulator. This behaviour was explained by the fact that nickel particles have the shape of 'thorns'; in addition, they are covered with a layer of graphene ensuring a high electrical conductivity of the composite in the working state. It sharply decreases upon heating due to the volume expansion of the polymer matrix and the loss of contact between the particles, thus providing an increase in the composite resistance.[108]

A significant drawback of these composites is that the thickness of their layer required for efficient protection should be ~10 μm, which is a significant fraction of the electrode thickness. As a result, the content of the active material in the battery decreases and the battery itself becomes heavier.[108]

Table 1. Composites of crystalline polymers with electrically conductive fillers.

Composite components (mass %)	δ, μm	T_c, °C	I_c	T_2, °C	Composition of the active mass (mass %)	Discharge		Ref.
						capacity, mA h g^{-1}	current density	
35% $LiFePO_4$/carbon black, 54% PVDF, 11% carbon black	3–4	80	–	–	95% lithiated Ni-Co-Mn oxide, 3% PVDF, 2% carbon black	–	–	106
30 vol.% spiky Ni oxide, 70% PE	15	70	10 000	80	80% $LiFePO_4$, 10% carbon black, 10% PVDF	140	0.1*C*	108
40% carbon black, 30% ER, 30% polyamide hardener	15	80	140	140	85% $LiCoO_2$, 7% AB, [a] 8% PTFE [b]	130	0.2*C*	124
1–7% PEO, 50–85% EVA, 10–30% AB [a]	10	70	>100	90	75% $LiFePO_4$, 20% AB, [a] 5% PTFE [b]	165	0.5*C*	125
10% carbon black, 90% PMMA	–	80	63	140	90% $LiCoO_2$, 3% AB, [a] 7% PVDF	100	2*C*	126
34% PVDF, 65% Ni, 1% carbon black	–	75	28	100	80% $LiFePO_4$, 10% carbon black, 10% PVDF	135	2*C*	127

Note. In the description of batteries, in order to normalize the capacity whose values vary greatly amond batteries, the charging (discharging) current is often expressed in *C* units. The value of *C* (*C*-rate) reflects the rate of charging (discharging) of a battery with respect to its maximum capacity. A current of 1*C* means that the entire battery is charged (discharged) in 1 h. For example, in a battery with a capacity of 100 A h, a current of 1*C* corresponds to 100 A, whereas *C*/2 refers to 50 A. Similarly, if the specific capacity is 140 mA h g^{-1}, then 1*C* corresponds to 140 mA g^{-1}, 0.2*C* = 28 mA g^{-1} (see Ref. 128). [a] AB is acetylene black. [b] PTFE is poly(tetrafluoroethylene).

An indisputable advantage of such systems is that they can potentially operate in a reversible manner.[129, 130] This property is not mentioned in articles dealing with the protection of LIBs, but commercially successful thermistors, *i.e.* analogues of thermistor layers, provide up to 1000 activations.

Internal or external short circuits are the main types of processes that cause emergency situations whose consequences are prevented using thermoresistive materials. All the stages characteristic of thermal runaway are realized in a short-circuited ordinary unprotected LIB, while the voltage decreases to 0 V. In a protected battery, after an external short circuit occurs, the temperature increases like in a conventional LIB, but it ceases to increase on reaching an intermediate value between T_c and T_2, while the voltage on its terminals differs from zero by the value of the Ohmic voltage drop IR, where I is the current in the system and R is the resistance of the protective layer. Thus, the short circuit mode becomes more like the battery discharge through a resistor.[102] In this case, heat release decreases, and if normal heat exchange between the battery and the environment exists, a constant cell temperature is established, hence no thermal runaway occurs.

Similar processes occur in the case of an internal short circuit caused, for example, by the growth of lithium dendrites through the separator or by penetration of a conductive object into the battery. A scheme of battery operation in case of internal short circuit caused by piercing it with a nail as an example is shown in Fig. 4. In the case of an unprotected battery, two paths for the passage of electric current from undamaged zones of the electrodes to the nail that short-circuits the battery are possible:

— through the active mass 'along' the aluminium current collector,

— along the shortest path from the active mass to the aluminium current collector and then through it.

Due to the large length and small thickness of the active mass, its resistance is much greater than that of aluminium, so the second option is realized. Thus, the electrical circuit of a battery with a nail can be represented as discharge to the nail acting as an external resistor. However, since the nail resistance is actually low and is comparable to the internal resistance of the battery, the short-circuit current reaches large values, thus causing thermal runaway.

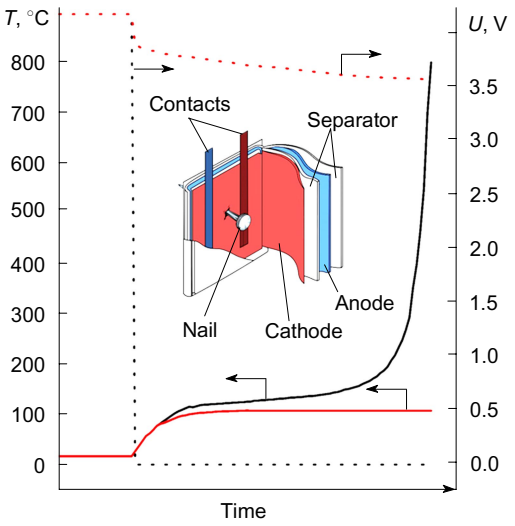


Figure 4. Scheme of the behaviour of batteries based on $LiCoO_2$: ordinary (black lines) and that protected by a thermoresistive layer (red lines) upon internal short circuit. The drawing was created by the authors based on data from Refs 103, 107.

In the case of a protected battery, the variants for the passage of electric current are corrected by the presence of a protective layer. Current can pass:

— through the active mass,

— through the protective layer,

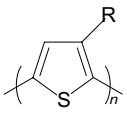
— from the active mass through the protective layer into aluminium.

When the battery operates in normal mode, the resistance of the protective layer is small, so the latter two options are identical to the typical current path in an unprotected battery, namely, from the active mass to the aluminium current collector and then through it. An internal short circuit causes the battery self-heating. However, at a temperature close to the actuation temperature of the protective sublayer, its resistance increases sharply, and the aluminium current collectors become as if 'disconnected' from the active mass. Therefore, the active mass that has a noticeable resistance remains the only conductor from the internal shunt (nail) to the active areas of electrodes. The short circuit current decreases and the behaviour of the battery resembles the discharge through a resistor. The battery temperature stabilizes near the transition temperature of the protective layer. This occurs due to the fact that at the initial moment of short circuit, the actuation temperature of protection is reached due to self-heating, *i.e.* the resistance increases. The increase in resistance causes a current decrease. As a result, cooling occurs and the resistance decreases. The decrease in resistance again leads to an increase in current, heating to the actuation temperature of protection and an increase in resistance, while the latter causes a decrease in current. In this case, the voltage on the battery terminals will have a non-zero value since the nail will be 'disconnected' by the protection resistance from the active mass. At the same time, it will not be equal to the initial value since battery capacity will be spent to maintain the actuation temperature, *i.e.* discharge through the resistance of the protective layer will occur.

3.2.3. Conductive polymers

The use of truly electrically conductive polymers can significantly decrease the thickness of the protective layer. As one can see from the data presented in Table 2, in contrast to crystalline polymer–conductive filler composites,[103, 115] the thickness of conductive polymer layers does not exceed 1 μm. Though various classes of electrically conductive polymers have a PTC, polythiophene derivatives (structures **1**–**4**) are mainly used to create protective layers for positively charged LIB electrodes.

Structures 1–4



1–4

R = n-$C_{12}H_{25}$ (**1**), n-C_8H_{17} (**2**), Bu^n (**3**), Ph (**4**)

Polyalkylthiophenes with substituents of various lengths were used in protective layers. It is known that as the length of the alkyl substituent increases, the transition temperature decreases.[103, 115] Taking into account that not only the temperature but also the I_c value itself change at the

Table 2. Compositions and characteristics of cathodes with layers of conductive polymers.

Layer composition	δ, μm (see [a])	T_c, °C	I_c	T_2, °C	Composition of the active mass (mass %)	Discharge		Ref.
						capacity, mA h g^{-1}	current density	
Poly(3-n-dodecylthiophene-2,5-diyl) (**1**)	0.4	–	3×10^4	100	80% $LiCoO_2$, 10% carbon black, 10% PVDF	157	0.25*C*	102
Poly(3-n-octylthiophene-2,5-diyl) (**2**)	1.0	–	667	110	85% $LiCoO_2$, 5% carbon black, 10% PVDF	147	0.25*C*	103
Poly(3-n-butylthiophene-2,5-diyl) (P_3BT) (**3**)	0.2	120	100	150	80% $Li[Ni_{0.5}Co_{0.2}Mn_{0.3}]O_2$, 10% carbon black, 10% PVDF	110	3*C*	115

[a] Layer thickness.

maximum actuation intensity (see Table 2), one can reach the required protective characteristics quite accurately by varying the nature of substituents.

Electrochemical tests in half-cells with a negative lithium electrode at room temperature showed no adverse effect of the protective layer on the properties of cells in the normal mode of operation, namely, the cycling stability and power remained unchanged. Li *et al.*[102] cycled elements with a current of 0.25*C* at room and slightly elevated (45 °C) temperatures for 100 and 200 cycles. The retention of the discharge capacity was 92.3 and 82.7% for the protected electrode, and 91.8 and 82.0% for the unprotected electrode, respectively. In another studys,[103] the stability upon cycling was estimated for a battery with a negative graphite electrode and a capacity of 3.43 A h. After 600 charge–discharge cycles with a current of 0.2*C*, the residual capacity was ~93.5% for both protected and unprotected samples. Similar results were obtained in article 115 after 100 charge–discharge cycles with a current of 0.5*C* (the residual capacity was >93%).

3.2.4. Thermoresistive conductive additives to the cathode material

Another strategy in the development of temperature-sensitive electrodes involves the incorporation of particles with a PTC as conductive additives to the electrode mass. The compositions and characteristics of composites and electrodes obtained using this scheme are presented in Table 3.

Kise *et al.*[131] began studies on cathode materials based on $LiCoO_2$ with addition of a PTC composite comprising high-density polyethylene as a matrix and carbon black as a conductive filler. Unfortunately, they did not disclose the composition of the thermoresistive composite and the full electrode composition. Short circuit and elevated temperature cycling tests were carried out with full-size batteries with capacities from 65 to 500 mA h with a graphite negative electrode.[132] The results are presented in Table 3.

Charge–discharge tests of batteries showed that addition of a thermoresistive composite had almost no effect on the discharge capacity up to a certain discharge rate. Kise *et al.*[132] discharged batteries with currents from 0.25*C* to 2*C*. The capacities of protected and unprotected samples

Table 3. Compositions and properties of thermoresistive conductive additives to the positive electrode.

PTC-composite components	T_c, °C	I_c	T_2, °C	Composition of the active mass (mass %)	Discharge		Ref.
					capacity [a]	current density	
$LiCoO_2$ – P3DT	80	10^5	120	$LiCoO_2$ – P3DT	125 mA h g^{-1}	1*C*	104
Poly(styrene sulfonate), poly(styrene sulfonate)/CB	100	10^6	120	80% $LiCoO_2$, 10% PVDF, 10% P3OPy/carbon black	150 mA h g^{-1}	40 mA g^{-1}	107
1–7% PEO, 50–85% EVA, 10–30% AB	70	100	95	67.5% $LiFePO_4$, 20% AB, 5% PTFE, 7.5 % PTC-composite	125 mA h g^{-1}	2*C*	125
High density PE, CB	120	8	140	$LiCoO_2$, 1% AB, 8% PVDF, 6–12% PTC-composite	65 mA h (96%)	1*C*	132
High density PE, CB	120	8	140	$LiCoO_2$, 0.25–1% AB, PVDF, 12% PTC-composite	38 mA h (80%)	3*C*	133
High density PE, CB	120	8	140	$LiCoO_2$, 1% AB, 8% PVDF, 12% PTC-composite	510 mA h (102%) 485 mA h (97%)	1*C*, 2*C*	134 134
High density PE, CB	120	8	140	82.5% $LiCoO_2$, 1% AB, 4.5% PVDF, 12% PTC-composite	478 mA h (95.6%)	2*C*	135
High density PE, CB	120	8	140	85% $LiCoO_2$, 1.5% AB, 4.5% PVDF, 9% PTC-composite	479 mA h (95.8%)	2*C*	135
High density PE, CB	120	8	140	86.5% $LiCoO_2$, 2% AB, 5.5% PVDF, 6% PTC-composite	500 mA h (100%)	2*C*	135

Note. The following designations are used: CB is carbon black; P3DT is poly(3-decylthiophene); P3OPy is poly(3-octylpyrrole). [a] The values in parentheses indicate the percentage of the discharge capacity of the nominal value at a given current density.

they obtained matched up to a rate of 1*C*. However, the higher internal resistance of protected batteries affected their operation in the case of discharge with higher currents: when discharged with currents of 1.5*C* and 2*C*, the unprotected sample showed ~96 and 78% of the nominal capacity, respectively, whereas the protected one showed 80 and 40%.

To improve the discharge characteristics of batteries, it was necessary to optimize the composition of the positive electrode by introducing an additional conductive additive, namely, acetylene black (AB).[125, 133] However, the latter adversely affects the protective properties of the electrode by reducing its resistance, including that at elevated temperatures. The corresponding studies were performed to determine the optimal ratio between AB and a PTC-composite.[131, 133, 134] The authors varied the AB content from 0.25 to 3%, while decreasing the content of the composite from 12 to 3%. With a decrease in the content of the PTC-composite and an increase in AB content, the electrochemical characteristics of the batteries improved: at a current of 2*C*, the discharge capacity of the protected battery was >95% of the nominal value, whereas that of the unprotected battery was 100%.

The external short circuit of batteries was done by connecting the positive and negative terminals. The unprotected sample showed a short circuit current of about 142*C*, while the protected batteries with various AB content gave no more than 21*C*.[133]

Zhong *et al.*[125] proposed another PTC-composite that consisted of PEO and EVA as a polymer matrix and carbon black as a conductive filler. As the temperature increases, this formulation increases the battery resistance starting from 60 °C. On reaching 85–95°C, the resistance increases ~100-fold. The charge–discharge characteristics of an electrode based on the active material comprising 67.5% $LiFePO_4$, 20% AB, 5% PTFE as a binder and 7.5% PTC composite did not differ from those of the unprotected electrode (75% $LiFePO_4$, 20% AB, 5% PTFE) at room temperature in the current range from 0.1*C* to 2*C*. The specific discharge capacity after 20 charge–discharge cycles at a current of 0.5*C* did not change and amounted to 160 mA h g^{-1} at room temperature. Only on heating to the transition temperature (90 °C), the material stopped to discharge and showed a discharge capacity of 0 mA h g^{-1} for a period of 20 cycles.

In contrast to the previous approaches, electrically conductive poly(3-octylpyrrole) (P3OPy) was used as a conductive additive to the electrode.[107] It was shown that transition of the polymer to the insulating state occurred at 100–120 °C.

$LiCoO_2$ and $LiCoO_2$–P3OPy electrodes demonstrated similar charge–discharge profiles with an average voltage of ~3.9 V at the same current density of 40 mA g^{-1} with comparable discharge capacities, namely, 147 and 150 mA h g^{-1}, respectively. A temperature increase to 120 °C resulted in a sharp decrease in the discharge capacity to 20 mA h g^{-1} in a protected sample. With a further temperature increase to 150 °C, the $LiCoO_2$–P_3OPy electrode behaved as if it was totally blocked, and voltage rapidly decreased to the lower limit (3.0 V) upon discharge. As a result, the battery did not demonstrate a noticeable discharge capacity.

Scaling to a full size battery (with a capacity of 3.5 A h) confirmed the feasibility of this protection method. The cycling stability (600 cycles) at a current of 1*C* was checked before safety testing. The residual capacity was 93.3% of the nominal value. Simulation of a short circuit (piercing with a needle) in two LIBs, one based on $LiCoO_2$–P_3OPy and one based on $LiCoO_2$, showed the superiority of the former: the surface temperature of the latter LIB abruptly increased to 523 °C after piercing it with the needle, the voltage dropped to 0 V, and ignition occurred, whereas these indicators were 44 °C and 3.8 V in the former LIB. No ignition occurred during short circuiting for 120 s.

Overcharge was chosen as yet another abnormal mode of operation to demonstrate the protection mechanism. Overcharge with a current of 0.4*C* was performed to a voltage of 10 V or 180% charge. In an unprotected sample at 159% charge, the voltage increased sharply to 9.98 V and the surface temperature increased to 510 °C. The voltage and temperature of a protected sample did not exceed 5.0 V and 100 °C, and these values remained at these levels until overcharge ceased.

A new thermosensitive cathode material, $LiCoO_2$–P3DT, was reported.[104] A P3DT coating with a thickness of 20 nm was deposited on $LiCoO_2$ particles with a size of 2–3 μm. The temperature range of resistance growth of this coating was 80–110 °C, and the resistance increased 10^5-fold. Charging–discharging with currents from 0.1*C* to 1*C* at room temperature did not show differences in the behaviour of LiCoO2–P3DT and pure $LiCoO_2$. The efficiency of the protective properties of a P3DT coating was demonstrated by discharging with a current of 40 mA g^{-1} at various temperatures.

3.2.5. Application of variable-resistance materials in negative electrodes

Modifying negative LIB electrodes with thermoresistive materials is much less common than modifying positive electrodes. Baginska *et al.*[136] studied the behaviour the behavior of batteries with a negative electrode coated with polyethylene or paraffin microspheres. It was found that the presence of up to 12 mg cm^{-2} PE microspheres did not affect the battery operation at a current load of 1*C*. Total blocking of discharge (loss of >98% of the initial capacity) at a temperature of >110 °C is achieved upon addition of as little as 3.5 mg cm^{-2} of the microspheres. For paraffin microspheres, the same indicator is achieved at a temperature of >65 °C and an amount of 2.9 mg cm^{-2}.

A negative graphite PTC electrode was studied in batteries based on $LiCoO_2$.[137] Polymer microspheres (PM) in the form of cyclopentane drops with a acrylonitrile–acrylate copolymer shell were used as the heat-sensitive additive. Due to the heat-sensitive properties of the PM, the graphite layer on the electrode swells under critical conditions, and the electrical contacts between the materials inside the active mass and between the active mass and the current lead are interrupted. Thus, the system resistance increases before the battery temperature approaches the temperature where thermal runaway starts. The polymer microspheres have a size of 4–20 μm and a transition temperature of 95–110 °C. The charge–discharge characteristics of batteries under normal conditions were found to be unaffected by the PM, and it was noted that batteries with the PM efficiently prevented the thermal runaway in tests for overcharge up to 10 V with a current of 1*C*, for thermal shock from 20 to 130 °C, and for external short circuit with a resistance of 80 mΩ.

4. Use of potentioresistive materials to prevent thermal runaway

4.1. Principles of operation of potentioresistive materials

The use of thermoresistive materials provides a sharp increase in the battery resistance at temperatures of $>100-180$ °C corresponding to the second stage of thermal runaway, *i.e.* the stage of heat accumulation.[78, 80, 96] At these temperatures, unwanted processes take place already (see Fig. 1), therefore actuation of thermoresistive protection can only reduce the likelihood of their further development.[43, 50] To protect a battery more completely, the protective mechanism needs to be actuated in the first stage of emergency development. In such case, the battery will potentially be able to maintain its operation after removal of the 'traumatic' impact. For example, voltage may become a trigger for actuating protective mechanisms.

It is known that intrinsically electrically conductive polymers conduct electricity only in a certain range of potentials as long as they are in a partially doped (oxidized) state. The electrical conductivity of such polymers reaches its maximum and then, when they are reduced or oxidized more completely, it decreases by several orders of magnitude [138–140] since the concentration of charge carriers (polarons) will either be very small or so high as to considerably reduce their mobility. This quality of conducting polymers can be used to protect LIB from undesirable consequences of abnormal operating modes, where the cell potential rather than temperature would be the trigger for actuating the protection. By analogy with thermoresistive materials, we will call such protective systems 'potentioresistive'. However, unlike thermoresistive protective components, which in fact act as fuses and operate when the temperature rises (*i.e.* after the start of irreversible processes in the battery), potentioresistive protective components are activated when the battery voltage goes out of range, which usually occurs before the onset of thermal runaway and related changes. There are two known approaches to battery protection using potentioresistive polymers. The first one is based on internal shunting of the battery, like the well-known electrolyte additives, *i.e.* redox shuttles, and the second one, in contrast, is based on interrupting the circuit, like a fuse.

4.2. Potentioresistive materials for controlling electronic conductivity

4.2.1. Separators

As noted above, conductive polymers are capable of changing their electrical conductivity depending on the electrode potential.[141] If we choose such a polymer that does not conduct electricity in the normal operating range of the battery voltage but begins to conduct it at higher voltages, and a layer of this polymer is placed between the positive and negative electrodes, *i.e.* in the separator, then as the polymer switches to the conductive state, a shunt is formed inside the battery through which the overcharge current will flow.[139] With such a separator, the battery can be protected from overcharge, since all additional charging capacity will pass through it without consequences, for example, undesirable electrochemical reactions.

The scheme of operation of a potentioresistive separator is presented in Fig. 5. In the normal operating mode, a separator behaves as a conventional polypropylene membrane. On reaching the oxidation potential of the electrically conductive polymer, electrical conductivity increases. Once the entire thickness of the separator becomes conductive, due to battery shunting, the voltage reaches a plateau and remains constant until the battery is disconnected from the charger.

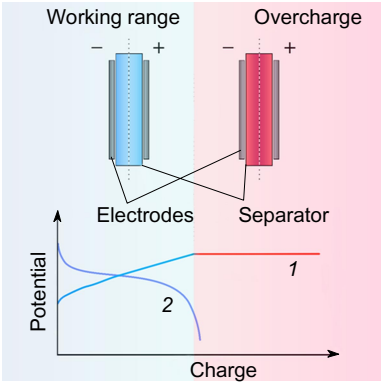


Figure 5. Scheme of a battery with a potentioresistive separator and approximate shape of charge-discharge curves; (*1*) charge curve with a voltage plateau upon overcharge, (*2*) discharge curve after overcharge; the area in blue corresponds to normal operation, while the area in pink corresponds to overcharge. The drawing was created by the authors based on data from Refs 142–144.

A mathematical model describing the applicability of electroactive polymers, such as PT, for overcharge protection was published in 2004.[145] According to the model, an overcharged cell behaves like a resistor with a resistance that varies depending on the distance between the electrodes. Upon discharge or chain interruption, the self-discharge of the battery results in the reduction of the conducting polymer and its transition to an insulating state. This converts the resistor into a non-conductive separator allowing the battery to perform normal charge and discharge cycles. The simplified model gives an equation that shows how the potential at which the cell is short-circuited depends on the current density, separator thickness, and electronic conductivity variation as a function of the oxidation state and the potential of the polymer.

Among the polymers used in potentioresistive separators, the following ones mentioned most frequantly can be distinguished:

— PT derivatives, for example P3BT (structure **3**), P3PT (structure **4**), a mixture of these polymers coated with poly[2-methoxy-5-(2-ethylhexyl)oxy-*p*-phenylene vinylene] (structure **5**), P3DT;

— polymeric derivatives of triphenylamine (structure **6**), for example, its copolymer with coumarin (structure **7**), polyaniline (structure **8**) and polyphenylene (structure **9**).

Structures 5–9

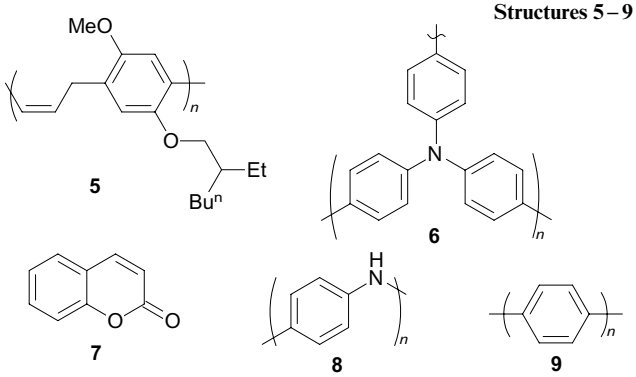


Table 4. Composition and properties of potentioresistive separators and cells based on them.

Separator composition	Electrolyte	Electrochemical system	Overcharge current, current density	Number of cycles	Ref.
P3DT in commercial PP/PE/PP separator	1 M $LiPF_6$, EC/DMC/EMC (1 : 1 : 1)	$LiFePO_4$| C	1*C*	100	143
Compressed membranes with the composition:					
60% poly(*p*-phenylene) + 40% PTFE	1 M $LiPF_6$, EC/DMC (1 : 1)	$LiMn_2O_4$| Li	25 mA g^{-1}	30	142
60% polyaniline + 40% PTFE	1 M $LiPF_6$, EC/DMC (1 : 1)	$LiMn_2O_4$| Li	25 mA g^{-1}	30	142
P3BT in Celgard separator combined with PDOF with terminal dimethylphenyl groups in Viledon separator	1 M $LiPF_6$, PC/EC/DMC (1 : 1 : 3)	$Li_{1.05}Mn_{1.95}O_4$| Li	*C*/6	20	147
P3BT coated with PDOF in fiber glass membranes modified dimethylphenyl groups	1 M $LiPF_6$, EC/DMC (1 : 1)	$LiNi_{1/3}Co_{1/3}Mn_{1/3}O_2$| Li	0.5*C*	200	148
		$LiFePO_4$| Li	0.5*C*	354	148
		$Li_{1.05}Mn_{1.95}O_4$ | Li	*C*/6	654	148
		$Li_{1.05}Mn_{1.95}O_4$ | Li	1*C*	500	148
P3BT in PDOF membrane with terminal dimethylphenyl groups in PEO	1 M $LiPF_6$, EC/DEC (1 : 1)	$LiNi_{1/3}Co_{1/3}Mn_{1/3}O_2$| Li	2/3*C*	1000	149
Copolymer of TPA with coumarin, membrane	1 M $LiPF_6$, EC/DMC (1 : 1)	$LiFePO_4$| Li	0.3*C*	7	150
A mixture of P3BT with P3PT coated with poly-[2-methoxy-5-(2-ethylhexyl)oxy-*p*-phenylenevinylene] in a commercial separator	1 M $LiPF_6$, EC/DEC (1 : 1)	$LiFePO_4$| Li	0.125 mA cm^{-1}	5	151
Membrane: 30% TPA, 30% Al_2O_3, 40% PTFE	1 M $LiPF_6$, EC/DMC (1 : 1)	$LiFePO_4$| Li	0.5*C*	40	152
P3BT in a commercial separator	1 M $LiPF_6$, EC/DMC/EMC (1 : 1 : 1)	$LiFePO_4$| $Li_4Ti_5O_{12}$	0.4 mA cm^{-1}	100	153
TPA in a polyvinyl alcohol membrane	1 M $LiPF_6$, EC/DEC (1 : 1)	$LiFePO_4$| Li	0.5*C*	50	154

Note. The following designations are used: P3BT is poly(3-butylthiophene), P3PT is poly(3-phenylthiophene), PDOF is poly(9,9-dioctylfluorene), TPA is triphenylamine, EC is ethylene carbonate, DMC is dimethyl carbonate, DEC is diethyl carbonate, EMC is ethyl methyl carbonate.

Among PT derivatives, P_3BT is studied most commonly due to its high redox potential and higher stability at highly negative potentials.[146]

Data on the electrochemical characteristics for overcharge of cells with potentioresistive separators, namely the type of the electrochemical system being protected, the overcharge current and the number of overcharge cycles are also presented in Table 4. Most often, this protection technology is offered for batteries based on $LiFePO_4$, since the redox transition potentials of the majority of electrically conducting polymers in separators do not exceed 4.0 V, which does not allow them to be used for higher-voltage systems because cell shunting begins in the operating range of potentials. However, some publications[142, 147–149] report separators that successfully protect batteries based on mixed oxides. Most publications give overcharge currents that do not exceed 1*C*, and the number of overcharging cycles increased from tens to hundreds and even thousands as the technology developed.

The best result was obtained for P_3BT coated with PDOF[148] and arranged within a commercial separator or glass fibre membrane (Table 4). Separators of this type exhibit excellent stability of up to 1000 recharge cycles by currents from *C*/6 to 1*C*.

4.2.2. Positive electrode

There are variants for protecting cathode materials using conductive polymers. These methods are based not on shunting but on interrupting the current when a certain potential is reached due to the property of polymers to pass from a conductive state to a non-conductive state at very high and very low potentials. So far, such protective systems have been tested only with low-voltage materials and represent a certain alternative to the shunting described above (see Section 4.2.1). However, in the future, polymer circuit breakers may also find use for high-voltage cathode materials. The use of shunting separators based on known electroconducting polymers is difficult for batteries with such materials due to the transition of the polymer to a conductive state, which is then preserved in a wide range of potentials within the operating voltage range.[155–157]As a result, the high-voltage cathode material cannot be charged fully.

Patel *et al.*[28] proposed poly(3-hexylthiophene-block-ethylene oxide) block copolymer as an additive to an electrode based on $LiFePO_4$ for protection against overdischarge. The dependence of electric conductivity on the electrode potential was established in the experiments. At potentials of the charge–discharge plateau of $LiFePO_4$ (3.4–3.6 V), the conductivity changed from 10^{-4} to 10^{-2} S cm^{-1}, while at the end-of-discharge potential (3.0 V) it was 10^{-7} S cm^{-1}, which allowed the material to stop the further discharge. Ultimately, due to the transition of poly(3-hexylthiophene-block-ethylene oxide) to an insulating state, potentioresistive protection against battery overdischarge was implemented.

Though a decrease in conductivity is also possible when the potential increases above a certain limit, conductive

polymers of only one class, namely, nickel complexes with poly[bis(salicylideneimine)] ligands, have been tested to date for LIB protection from overcharging.[139] The range of potentials at which the resistance of these polymers is the smallest is 3.2 – 4.4 V *versus* the lithium reference electrode. This range is suitable for protection of the majority of commercial cathode materials; however, an example of such protection is known only for an electrode based on lithium ferrophosphate. The poly[Ni(MeOSalen)] complex was used. Its resistance in reduced state amounted to 40 000 Ω.[105] As the potential changes to 3.60 – 3.70 V, the polymer is oxidized and its resistanse decreases to 40 Ω, but upon more complete oxidation it rises again to 400 – 1000 Ω at potentials of >4.20 V. To demonstrate the protective properties of this polymer, batteries with a positive electrode based on $LiFePO_4$ and a protective layer of poly[Ni(MeOSalen)] 1 μm thick located between the active mass and the current lead were overcharged in galvanostatic mode. Overcharging was carried out by a current of 0.25*C* to 5.00 V and by a current of 1*C* to 6 V. It was shown that at low charge current, poly[Ni(MeOSalen)] increases the electrode resistance to overcharge: after 25 overcharges, the specific discharge capacity of a protected electrode was ~116 mA h g^{-1}, while that of an unprotected one was 75 mA h g^{-1}. At a higher charging rate, poly[Ni(MeOSalen)] prevents the excessive release of gaseous products of electrolyte decomposition, while an increase in the internal resistance of the battery hampers the possible thermal runaway.

The resistance of polymeric nickel complexes with salen-type ligands can change either reversibly or irreversibly. It was shown for *N*,*N*′-ethylenebis(3-methyl salicylideneiminato)nickel(II) and poly[Ni(MeOSalen)] as examples [139] that a five-minute exposure at potentials above 4.1, 4.2 and 4.6 V, respectively, resulted in almost complete loss of conductivity, which can be used for battery protection against potentiostatic overcharging at 5 V.

Simulation of processes that occur during overcharging showed that protection by means of potentioresistive layers should be effective in various overcharging modes and for various cell configurations.[158] Among materials suitable for use as potentioresistive protective layers, mention may also be made of electrically conductive polymers with a narrow range of electrical conductivity coinciding with the potential range of LIB operation. Materials that potentially meet this requirement are known from studies aimed at solving problems other than protection of batteries. The most frequent literature sources include studies of various thiophene derivatives, complexes of transition metals with salen-type ligands, and their combinations. A summary of known polymers (structures **10** – **22**) for which specific electrical conductivity measurements were performed *in situ* is presented in Table 5.

As analysis of presented data shows, the majority of compounds do not have a sufficiently narrow range of conduction potentials to meet the applicability criteria as protective layers for positive LIB electrodes. For most commercial electrode materials, polymer nickel complexes with salen-type ligands are most suitable in terms of the potential range.

It should be noted that almost all of the polymers mentioned above were tested in non-aqueous media based on acetonitrile and dichloromethane, rather than in the electrolytes used in the LIB. Therefore, the potentials presented in Table 5 were converted to the lithium reference electrode without taking the solvent effects into account, *i.e.* tentative data are given that require experimental adjustment in studies of particular polymers in particular electrolytes.

Structures 10 – 22

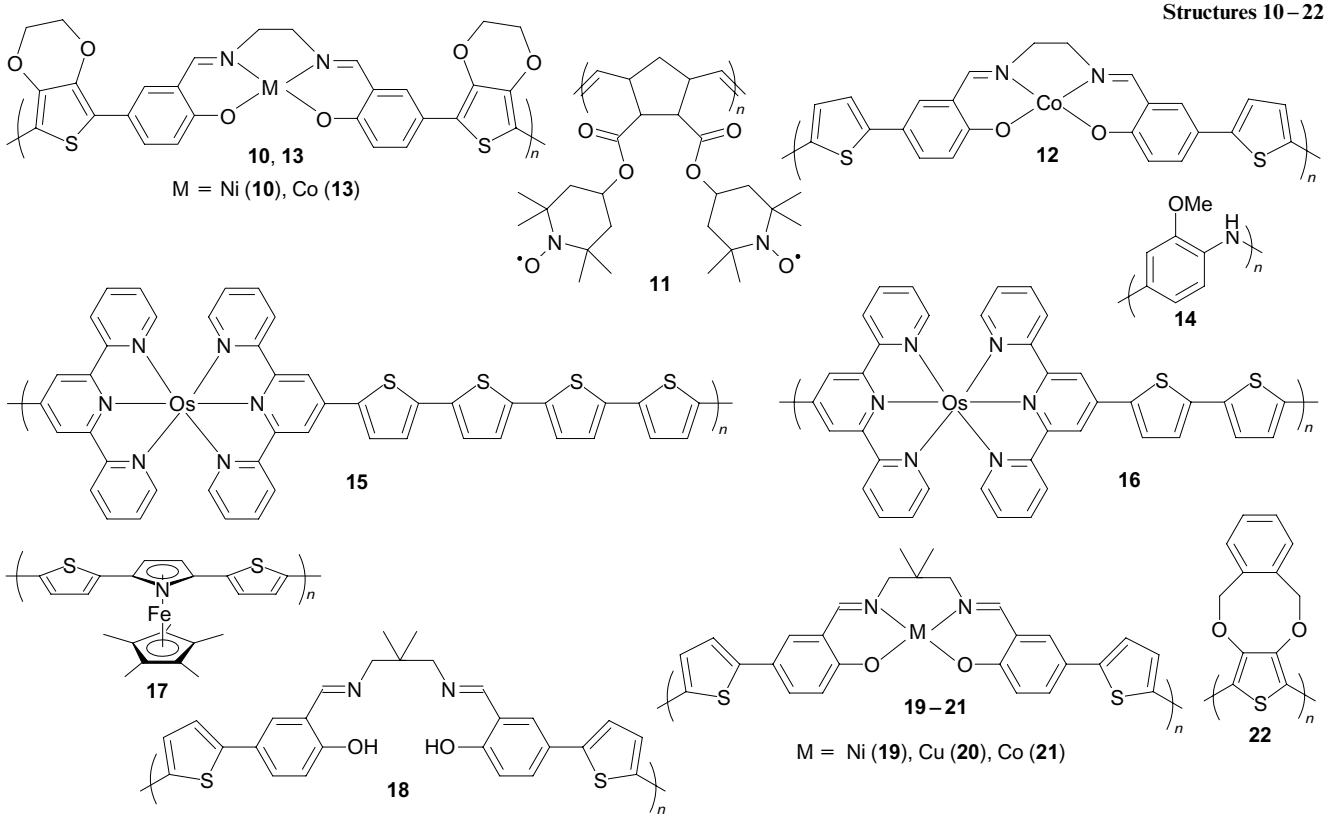


Table 5. Properties of potentioresistive polymers.

Compounds	Conductivity, S cm^{-1}	Range of potentials, V	Range of potentials, Li|Li$^+$, V	Electrolyte	Ref.
Copolymer of *N*,*N*′-ethylenebis(salicilydeneiminato)-nickel with 3,4-(ethylenedioxy)thiophene (**10**)	100	−0.45 to 0.85	2.80 – 4.10	0.1 M $C_{16}H_{36}F_6NP$, AN	138
Poly[2,3-bis(2,2,6,6-tetramethyl-*N*-oxyl-4-oxycarbonyl)norbornene] (**11**)	10^{-5}	0.20 to 0.50	3.45 – 3.95	0.1 M $C_{16}H_{36}F_6NP$, AN	140
Polymer of *N*,*N*′-ethylenebis[5-(2-thienyl)-salicilydeneiminato]cobalt (**12**)	40	−0.5 to 0.75 (see [a])	2.75 – 4.00	0.1 M $C_{16}H_{36}F_6NP$, AN	159
Polymer of *N*,*N*′-ethylenebis{5-[2-(3,4-ethylenedioxy)-thienyl]salicylideneiminato}cobalt (**13**)	240	−1.3 to 0.4 (see [a])	1.95 – 3.65	0.1 M $C_{16}H_{36}F_6NP$, AN	159
Poly(2-methoxyaniline) (**14**)	8.5	−0.2 to 0.7	3.042 – 3.942	1 M H_2SO_4	160
Poly[bis(2,2′:3′,2″-terpyridine)-4′-yl]tetrakis-(thiophene-2,5-diyl)]osmium (**15**)	10^{-4}	0.3 – 0.7	3.55 – 3.95	0.1 M $C_{16}H_{36}F_6NP$, AN + 5% $C_4H_{10}BF_3O$	161
Poly[bis(2,2′:3′,2″-terpyridine)-4′-yl]bis(thiophene-2,5-diyl)]osmium (**16**)	0.0016	0.3 – 1.1 (see [a])	3.55 – 4.35	0.1 M $C_{16}H_{36}F_6NP$, AN	162
Poly[2,5-bis(thiophene-2,5-diyl)-1′,2′,3′,4′,5′-pentamethyl-1-azaferrocene] (**17**)	20	−0.4 to 1.1 (see [a])	2.85 – 4.35	0.1 M $C_{16}H_{36}F_6NP$, CH_2Cl_2	163
Poly[*N*,*N*′-(2,2-dimethylprop-1,3-diyl)bis-(thiophene-2,5-diyl)salicylideneimine] (**18**)	8×10^{-6}	−0.75 to 1.25 (see [a])	2.50 – 4.50	0.1 M $C_{16}H_{36}F_6NP$, CH_2Cl_2	164
Poly{[*N*,*N*′-(2,2-dimethylprop-1,3-diyl)bis-(thiophene-2,5-diyl)salicylideneiminato]nickel} (**19**)	0.025	−0.7 to 1.25 (see [a])	2.50 – 4.50	0.1 M $C_{16}H_{36}F_6NP$, CH_2Cl_2	164
Poly{[*N*,*N*′-(2,2-dimethylprop-1,3-diyl)bis-(thiophene-2,5-diyl)salicylideneiminato]copper} (**20**)	0.01	−0.75 to 1.25 (see [a])	2.50 – 4.50	0.1 M $C_{16}H_{36}F_6NP$, CH_2Cl_2	164
Poly{[*N*,*N*′-(2,2-dimethylprop-1,3-diyl)bis-(thiophene-2,5-diyl)salicylideneiminato]cobalt} (**21**)	0.001	−0.75 to 1.25 (see [a])	2.50 – 4.50	0.1 M $C_{16}H_{36}F_6NP$, CH_2Cl_2	164
Poly{[3,4-[di(oxymethyl)-*o*-xylilene]-thiophene-2,5-diyl} (**22**)	0.5	−1.0 to 1.5	–	0.1 M $C_{16}H_{36}F_6NP$, AN	165

Note. The reference electrodes used were as follows: Fc/Fc$^+$ for compounds **10** – **13** and **15** – **21**, saturated calomel electrode for compound **14**, and silver wire for compound **22**. Electrolytes: $C_{16}H_{36}F_6NP$ is tetrabutylammonium hexafluorophosphate, $C_4H_{10}BF_3O$ is boron trifluoride diethyl etherate, AN is acetonitrile. [a] The conductivity range is limited by the authors rather than determined from a conductivity decrease below a threshold value.

5. Conclusion

It has been shown in the part of the review dealing with the mechanism of thermal runaway that the first stage (onset of overheating) can be caused by overcharge or internal short circuit, for example, due to the intergrowth of lithium dendrites. Heat-resistant protective layers begin to operate only when a temperature that is critical for them is reached. The potentioresistive layers protect a LIB before a sharp rise in temperature begins, which is preferable since this sharp rise leads to the battery failure.

However, situations are possible where the temperature itself 'triggers' the thermal runaway, for example, in case of overheating or extensive damage to the battery. In this case, the efficiency of a potentioresistive layer may be insufficient. It is likely that combining both protection options would be most efficient.

The following variants of such a combination can be suggested.

1. If various potentio- and thermoresistant compounds are used, they can be arranged on the electrode either layer-by-layer, by placing the thermo-resistive layer on the current collector and the potentioresistive layer on top of the former, or as one layer comprising a mixture or a bifunctional material. Thus, in a two-layer design, the active mass of the positive electrode is separated from the current lead by layers with potentio- and thermoresistive properties; in a single-layer design, a composite is created in which the ratio of components is tuned to obtain the optimal protective characteristics. The protection mechanism is quite clear in both cases: if the temperature or voltage increases, either the first or the second component works.

2. Since multi-component mixtures or multilayer coatings always increase the cost of manufacturing a battery, it is preferable to select an electrically conductive polymer that has both potentio- and thermoresistive properties. It has been shown [116] that polyNi(MeOSalen)] previously considered as a potentioresistive polymeric complex has a PTC with a transition temperature of ~220 °C that corresponds to the last stages of thermal runaway, so the efficiency of thermoresistive protection by this polymer is low. However, changing the nature and size of the substituents in the ligand structure might provide a solution that would allow shifting the transition temperature to lower values acceptable for battery protection, while maintaining the potentioresistive properties of the material.

The review was prepared with financial support of the Russian Foundation for Basic Research (Project No. 20-13-50195).

The authors are grateful to A.A.Vereshchagin and D.A.Luk'yanov for assistance in the preparation of illustrative materials for this review.

6. List of abbreviations and symbols

AN — acetonitrile,
AB — acetylene black,
CB — carbon black,
DMC — dimethyl carbonate,
DEC — diethyl carbonate,
EC — ethylene carbonate,
ER — epoxy resin,
EVA — poly(ethylene-co-vinyl acetate),
I — current flowing in the system,
Ic — response intensity,
LIB — lithium-ion batteries,
P3BT — poly(3-butylthiophene),
PDFE — poly(1,1-difluoroethylene),
PDOF — poly(9,9-dioctylfluorene),
P3DT — poly(3-decylthiophene),
PC — propylene carbonate,
PM — polymer microspheres,
PMMA — poly(methyl methacrylate),
P3OPy — poly(3-octylpyrrole),
PP — polypropylene,
PTC — positive temperature coefficient,
P3PT — poly(3-phenylthiophene),
PTFE — poly(tetrafluoroethylene),
TPA — triphenylamine,
PT — polythiophene,
PE — polyethylene,
PEO — poly(ethylene oxide),
R — protective layer resistance,
SEI — solid electrolyte interface,
poly[Ni(MeOSalen)] — N,N'-ethylenebis(3-methoxysalicylideneiminato)nickel(II),
Tc — transition temperature,
Tm — melting point,
Tr — room temperature, (20 ± 5) °C,
δ — layer thickness.

7. References

1. E.V.Makhonina, L.S.Pechen, V.V.Volkov, A.M.Rumyantsev, Y.M.Koshtyal, A.O.Dmitrienko, Y.A.Politov, V.S.Pervov, I.L.Eremenko. *Russ. Chem. Bull.*, **68**, 301 (2019)
2. L.S.Pechen, E.V.Makhonina, A.M.Rumyantsev, Y.M.Koshtyal, V.V.Volkov, A.S.Goloveshkin, V.S.Pervov, I.L.Eremenko. *Russ. Chem. Bull.*, **68**, 293 (2019)
3. D.Lee. Status Report on High Energy Density Batteries Project; URL: https://www.cpsc.gov/s3fspublic/High_Energy_-Density_Batteries_Status_Report_2_12_18.pdf (2018) (last accessed 17.02.20220
4. L.Lu, X.Han, J.Li, J.Hua, M.Ouyang. *J. Power Sources*, **226**, 272 (2013)
5. D.Aurbach, K.Gamolsky, B.Markovsky, Y.Gofer, M.Schmidt, U.Heider. *Electrochim. Acta*, **47**, 1423 (2002)
6. Y.Matsuo, K.Fumita, T.Fukutsuka, Y.Sugie, H.Koyama, K.Inoue. *J. Power Sources*, **119**–**121**, 373 (2003)
7. S.Komaba, B.Kaplan, T.Ohtsuka, Y.Kataoka, N.Kumagai, H.Groult. *J. Power Sources*, **119**–**121**, 378 (2003)
8. K.M.Abraham, D.M.Pasquariello, E.B.Willstaedt. *J. Electrochem. Soc.*, **137**, 1856 (1990)
9. G.Halpert, S.Surampudi, D.Shen, C.K.Huang, S.Narayanan, E.Vamos, D.Perrone. *J. Power Sources*, **47**, 287 (1994)
10. L.M.Moshurchak, C.Buhrmester, J.R.Dahn. *J. Electrochem. Soc.*, **155**, A129 (2008)
11. L.M.Moshurchak, W.M.Lamanna, M.Bulinski, R.L.Wang, R.R.Garsuch, J.Jiang, D.Magnuson, M.Triemert, J.R.Dahn. *J. Electrochem. Soc.*, **156**, A309 (2009)
12. X.M.Feng, X.P.Ai, H.X.Yang. *J. Appl. Electrochem.*, **34**, 1199 (2004)
13. S.Tobishima, Y.Ogino, Y.Watanabe. *J. Appl. Electrochem.*, **33**, 143 (2003)
14. X.L.Yao, S.Xie, C.H.Chen, Q.S.Wang, J.H.Sun, Y.L.Li, S.X.Lu. *J. Power Sources*, **144**, 170 (2005)
15. H.F.Xiang, Q.Y.Jin, C.H.Chen, X.W.Ge, S.Guo, J.H.Sun. *J. Power Sources*, **174**, 335 (2007)
16. Y.E.Hyung, D.R.Vissers, K.Amine. *J. Power Sources*, **119**, 383 (2003)
17. J.Kalhoff, G.-T.Kim, S.Passerini, G.B.Appetecchi. *J. Power Energy Eng.*, **4**, 10 (2016)
18. D.H.C.Wong, J.L.Thelen, Y.Fu, D.Devaux, A.A.Pandya, V.S.Battaglia, N.P.Balsara, J.M.DeSimone. *Proc. Natl. Acad. Sci. USA*, **111**, 3327 (2014)
19. R.Kanno, M.Murayama. *J. Electrochem. Soc.*, **148**, A742 (2001)
20. Y.Inaguma, C.Liquan, M.Itoh, T.Nakamura, T.Uchida, H.Ikuta, M.Wakihara. *Solid State Commun.*, **86**, 689 (1993)
21. V.Thangadurai, S.Narayanan, D.Pinzaru. *Chem. Soc. Rev.*, **43**, 4714 (2014)
22. U.V.Alpen, A.Rabenau, G.H.Talat. *Appl. Phys. Lett.*, **30**, 621 (1977)
23. G.B.Kunshina, O.G.Gromov, A.P.Kuz'min, E.B.Seitenova, E.P.Lokshin, V.T.Kalinnikov. *Russ. J. Appl. Chem.*, **77**, 915 (2004)
24. F.Croce, G.B.Appetecchi, L.Persi, B.Scrosati. *Nature (London)*, **394**, 456 (1998)
25. P.Arora, Z.Zhang. *Chem. Rev.*, **104**, 4419 (2004)
26. C.M.Costa, E.Lizundia, S.Lanceros-Méndez. *Prog. Energy Comb. Sci.*, **79**, 100846 (2020)
27. T.-H.Le, Y.Kim, H.Yoon. *Polymers*, **9**, 150 (2017)
28. S.N.Patel, A.E.Javier, N.P.Balsara. *ACS Nano*, **7**, 6056 (2013)
29. Q.Wang, P.Ping, X.Zhao, G.Chu, J.Sun, C.Chen. *J. Power Sources*, **208**, 210 (2012)
30. C.Mikolajczak, M.Kahn, K.White, R.T.White. *Lithium-ion Batteries Hazard and Use Assessment Final Report*; URL: https://www.nfpa.org/-/media/Files/News-and-Research/Fire-statistics-and-reports/Hazardous-materials/rflithiumionbatteriesshazard.ashx (2011) (last accessed 17.02.2022)
31. Q.Wang, B.Mao, S.I.Stoliarov, J.Sun. *Prog. Energy Comb. Sci*, **73**, 95 (2019)
32. X.Feng, S.Zheng, D.Ren, X.He, L.Wang, H.Cui, X.Liu, C.Jin, F.Zhang, C.Xu, H.Hsu, S.Gao, T.Chen, Y.Li, T.Wang, H.Wang, M.Li, M.Ouyang. *Appl. Energy*, **246**, 53 (2019)
33. S.Zhang, Z.Shen, Y.Lu. *Acta Phys. — Chim. Sinica*, **37**, 1 (2021)
34. Z.Wang, J.Yuan, X.Zhu, H.Wang, L.Huang, Y.Wang, S.Xu. *J. Energy Chem.*, **55**, 484 (2021)
35. Z.Zhang, Z.Du, Z.Han, H.Wang, S.Wang. *Int. J. Energy Res.*, **44**, 11840 (2020)
36. D.Spiers. In *McEvoy's Handbook of Photovoltaics: Fundamentals and Applications*. (Ed. S.A.Kalogirou). (San Diego, US: Academic Press, 2017). P. 789
37. T.Ma, S.Wu, F.Wang, J.Lacap, C.Lin, S.Liu, M.Wei, W.Hao, Y.Wang, J.W.Park. *ACS Appl. Mater. Interfaces*, **12**, 56086 (2020)
38. D.Juarez-Robles, A.A.Vyas, C.Fear, J.A.Jeevarajan, P.P.Mukherjee. *J. Electrochem. Soc.*, **167**, 090558 (2020)
39. X.Lai, C.Jin, W.Yi, X.Han, X.Feng, Y.Zheng, M.Ouyang. *Energy Storage Mater.*, **35**, 470 (2021)
40. D.Ren, X.Feng, L.Liu, H.Hsu, L.Lu, L.Wang, X.He, M.Ouyang. *Energy Storage Mater.*, **34**, 563 (2021)
41. T.G.Zavalis, M.Behm, G.Lindbergh. *J. Electrochem. Soc.*, **159**, A848 (2012)

42. K.Liu, Y.Liu, D.Lin, A.Pei, Y.Cui. *Sci. Adv.*, **4**, 9820 (2018)
43. Y.Chen, Y.Kang, Y.Zhao, L.Wang, J.Liu, Y.Li, Z.Liang, X.He, X.Li, N.Tavajohi, B.Li. *J. Energy Chem.*, **59**, 83 (2021)
44. N.Mao, Z.R.Wang, Y.H.Chung, C.M.Shu. *Appl. Therm. Eng.*, **163**, 114147 (2019)
45. D.Ren, X.Feng, L.Lu, X.He, M.Ouyang. *Appl. Energy*, **250**, 323 (2019)
46. D.Belov, M.-H.Yang. *Solid State Ionics*, **179**, 1816 (2008)
47. B.Mao, H.Chen, Z.Cui, T.Wu, Q.Wang. *Int. J. Heat Mass Trans.*, **122**, 1103 (2018)
48. D.Wang, L.Zheng, X.Li, G.Du, Z.Zhang, Y.Feng, L.Jia, Z.Dai. *Energies*, **13**, 3885 (2020)
49. D.Ouyang, Y.He, M.Chen, J.Liu, J.Wang. *J. Therm. Anal. Calorim.*, **132**, 65 (2018)
50. X.Feng, D.Ren, X.He, M.Ouyang. *Joule*, **4**, 743 (2020)
51. E.Sahraei, J.Campbell, T.Wierzbicki. *J. Power Sources*, **220**, 360 (2012)
52. P.G.Balakrishnan, R.Ramesh, T.Prem Kumar. *J. Power Sources*, **155**, 401 (2006)
53. Q.Wang, P.Ping, J.Sun. *Nonlinear Dynamics*, **61**, 763 (2010)
54. K.Kumaresan, G.Sikha, R.E.White. *J. Electrochem. Soc.*, **155**, A164 (2008)
55. Y.Huang, Y.Lu, R.Huang, J.Chen, F.Chen, Z.Liu, X.Yu, A.P.Roskilly. *Energy Proc.*, **142**, 4029 (2017)
56. M.-S.Wu, K.H.Liu, Y.-Y.Wang, C.-C.Wan. *J. Power Sources*, **109**, 160 (2002)
57. X.Feng, M.Ouyang, X.Liu, L.Lu, Y.Xia, X.He. *Energy Storage Mater.*, **10**, 246 (2018)
58. P.Jindal, J.Bhattacharya. *J. Electrochem. Soc.*, **166**, A2165 (2019)
59. P.V.Chombo, Y.Laoonual. *J. Power Sources*, **478**, 228649 (2020)
60. L.Huang, Z.Zhang, Z.Wang, L.Zhang, X.Zhu, D.D.Dorrell. *J. Energy Storage*, **25**, 100811 (2019)
61. D.Guo, L.Sun, X.Zhang, P.Xiao, Y.Liu, F.Tao. In *Proceeding of the 2nd IEEE Conference on Energy Internet and Energy System Integration (EI2)*. (Beijing, China, 2018). P. 1
62. R.Spotnitz, J.Franklin. *J. Power Sources*, **113**, 81 (2003)
63. N.K.Thangavel, S.Mundhe, M.M.Islam, G.Newaz, L.M.R.Arava. *J. Electrochem. Soc.*, **167**, 16 (2020)
64. G.Guo, B.Long, B.Cheng, S.Zhou, P.Xu, B.Cao. *J. Power Sources*, **195**, 2393 (2010)
65. G.-H.Kim, A.Pesaran, R.Spotnitz. *J. Power Sources*, **170**, 476 (2007)
66. P.Lyu, X.Liu, J.Qu, J.Zhao, Y.Huo, Z.Qu, Z.Rao. *Energy Storage Mater.*, **31**, 195 (2020)
67. Y.Liu, R.Huo, H.Qin, X.Li, D.Wei, T.Zeng. *J. Energy Storage*, **31**, 101643(2020)
68. C.Essl, A.W.Golubkov, A.Fuchs. *J. Electrochem. Soc.*, **167**, 130742 (2020)
69. P.Hundekar, R.Jain, A.S.Lakhnot, N.Koratkar. *J. Appl. Phys.*, **128**, 010903 (2020)
70. S.Wang, K.Rafiz, J.Liu, Y.Jin, J.Y.S.Lin. *Sustain. Energy Fuels*, **4**, 2342 (2020)
71. M.Gao, H.Li, L.Xu, Q.Xue, X.Wang, Y.Bai, C.Wu. *J. Energy Chem.*, **59**, 666 (2021)
72. J.Wen, Y.Yu, C.Chen. *Mater. Express*, **2**, 197 (2012)
73. J.Arai, Y.Okada, T.Sugiyama, M.Izuka, K.Gotoh, K.Takeda. *J. Electrochem. Soc.*, **162**, A952 (2015)
74. M.N.Richard, J.R.Dahn. *J. Electrochem. Soc.*, **146**, 2068 (1999)
75. G.Gachot, S.Grugeon, G.G.Eshetu, D.Mathiron, P.Ribière, M.Armand, S.Laruelle. *Electrochim. Acta*, **83**, 402 (2012)
76. J.Jiang, J.R.Dahn. *Electrochim. Acta*, **49**, 4599 (2004)
77. M.N.Richard, J.R.Dahn. *J. Electrochem. Soc.*, **146**, 2078 (1999)
78. A.Kriston, A.Kersys, A.Antonelli, S.Ripplinger, S.Holmstrom, S.Trischler, H.Döring, A.Pfrang. *J. Power Sources*, **454** (2020)
79. C.Zhang, H.Li, S.Wang, Y.Cao, H.Yang, X.Ai, F.Zhong. *J. Energy Chem.*, **44**, 33 (2020)
80. E.P.Roth, D.H.Doughty, D.L.Pile. *J. Power Sources*, **174**, 579 (2007)
81. P.Ping, Q.Wang, P. Huang, J.Sun, C.Chen. *Appl. Energy*, **129**, 261 (2014)
82. Y.S.Duh, X.Liu, X.Jiang, C.S.Kao, L.Gong, R.Shi. *J. Energy Storage*, **30**, 101422 (2020)
83. Z.Wei, H.Cao, C.Liang, Z.Wang, L.Feng, Q.Wang, J.Sun. *J. Electrochem. Soc.*, **168**, 020522 (2021)
84. K.Yang, Z.Shan, X.Liu, L.Tan, S.Wang. *Energy Technol.*, **9**, 2000816 (2021)
85. P.V.Chombo, Y.Laoonual. *J. Power Sources*, **478**, 228649 (2020)
86. S.-M.Bak, E.Hu, Y.Zhou, X.Yu, S.D.Senanayake, S.-J.Cho, K.-B.Kim, K.Y.Chung, X.-Q.Yang, K.-W.Nam. *ACS Appl. Mater. Interfaces*, **6**, 22594 (2014)
87. J.Duan, X.Tang, H.Dai, Y.Yang, W.Wu, X.Wei, Y.Huang. *Electrochem. Energy Rev.*, **3**, 1 (2020)
88. A.Mauger, C.M.Julien. *Ionics*, **23**, 1933 (2017)
89. E.P.Roth, C.J.Orendorff. *Interface Magaz.*, **21**, 45 (2012)
90. X.Tian, Y.Yi, B.Fang, P.Yang, T.Wang, P.Liu, L.Qu, M.Li, S.Zhang. *Chem. Mater.*, **32**, 9821 (2020)
91. C.M.Costa, E.Lizundia, S.Lanceros-Méndez. *Prog. Energy Comb. Sci.*, **79** (2020)
92. N.Mohamed, N.K.Allam. *RSC Adv.*, **10**, 21662 (2020)
93. S.S.Zhang. *J. Power Sources*, **164**, 351 (2007)
94. Z.Lu, F.Sui, Y.E.Miao, G.Liu, C.Li, W.Dong, J.Cui, T.Liu, J.Wu, C.Yang. *J. Energy Chem.*, **58**, 170 (2021)
95. C.M.Costa, S.Lanceros-Mendez. *Curr. Opin. Electrochem.*, **29**, 100752 (2021)
96. H.Liao, H.Zhang, G.Qin, H.Hong, Z.Li, Y.Lin, L.Li. *Macromol. Mater. Eng.*, **302**, 1700241 (2017)
97. W.Ni, D.Yang, J.Cheng, X.Li, Q.Guan, B.Wang. *RSC Adv.*, **6**, 52966 (2016)
98. M.Abudakka, D.S.Decker, L.T.Sutherlin, D.Teeters. *Int. J. Hydrogen Energy*, **39**, 2988 (2014)
99. H.Yang, Z.Liu, B.K.Chandran, J.Deng, J.Yu, D.Qi, W.Li, Y.Tang, C.Zhang, X.Chen. *Adv. Mater.*, **27**, 5593 (2015)
100. G.Zheng, W.Zhang, X.Huang. *Chemistry Select*, **3**, 11573 (2018)
101. O.S.Mendoza-Hernandez, H.Ishikawa, Y.Nishikawa, Y.Maruyama, M.Umeda. *J. Power Sources*, **280**, 499 (2015)
102. H.Li, X.Zhang, C.Zhang, Y.Cao, H.Yang, X.Ai, F.Zhong. *Energy Technol.*, **8**, 2000365 (2020)
103. W.Ji, F.Wang, D.Liu, J.Qian, Y.Cao, Z.Chen, H.Yang, X.Ai. *J. Mater. Chem. A*, **4**, 11239 (2016)
104. L.Xia, S.-L.Li, X.-P.Ai, H.-X.Yang, Y.-L.Cao. *Energy Environ. Sci.*, **4**, 2845 (2011)
105. E.V.Beletskii, A.A.Fedorova, D.A.Lukyanov, A.Y.Kalnin, V.A.Ershov, S.E.Danilov, D.V.Spiridonova, E.V.Alekseeva, O.V.Levin. *J. Power Sources*, **490**, 229548 (2021)
106. H.Z.Jin, X.F.Han, P.M.Radjenovic, J.H.Tian, J.F.Li. *J. Phys.Chem. C*, **125**, 1761 (2021)
107. H.Li, F.Wang, C.Zhang, W.Ji, J.Qian, Y.Cao, H.Yang, X.Ai. *Energy Storage Mater.*, **17**, 275 (2019)
108. Z.Chen, P.C.Hsu, J.Lopez, Y.Li, J.W.F.To, N.Liu, C.Wang, S.C.Andrews, J.Liu, Y.Cui, Z.Bao. *Nat. Energy*, **1**, 15009 (2016)
109. M.B.Heaney. *Appl. Phys. Lett.*, **69**, 2602 (1996)
110. M.Hindermann-Bischoff, F.Ehrburger-Dolle. *Carbon*, **39**, 375 (2001)
111. J.-Z.Liang, Q.-Q.Yang. *Composites, Part B*, **114**, 457 (2017)
112. M.Zhang, W.Jia, X.Chen. *J. Appl. Polym. Sci.*, **62**, 743 (1996)
113. A.Kono, K.Shimizu, H.Nakano, Y.Goto, Y.Kobayashi, T.Ougizawa, H.Horibe. *Polymer*, **53**, 1760 (2012)
114. H.Xu. In *Polymer Nanocomposites. Electrical and Thermal Properties*. (Eds X.Huang, C.Zhi). (Cham: Springer, 2016). P. 83

115. H.Zhang, J.Pang, X.Ai, Y.Cao, H.Yang, S.Lu. *Electrochim. Acta*, **187**, 173 (2016)
116. E.Beletskii, V.Ershov, S.Danilov, D.Lukyanov, E.Alekseeva, O.Levin. *Polymers*, **12**, 2925 (2020)
117. Y.Wang, M.F.Rubner. *Synth. Met.*, **39**, 153 (1990)
118. M.T.Loponen, T.Taka, J.Laakso, K.Väkiparta, K.Suuronen, P.Valkeinen, J.E.Österholm. *Synth. Met.*, **41**, 479 (1991)
119. Q.Pei, O.Inganäs, G.Gustafsson, M.Granström, M.Andersson, T.Hjertberg, O.Wennerström, J.E.Österholm, J.Laakso, H.Järvinen. *Synth. Met.*, **55**, 1221 (1993)
120. L.Szabo, G.Čík, J.Sitek, M.Seberíni. *Synth. Met.*, **88**, 79 (1997)
121. H.Koizumi, H.Dougauchi, T.Ichikawa. *J. Phys. Chem. B*, **109**, 15288 (2005)
122. E.Ando, S.Onodera, M.Iino, O.Ito. *Carbon*, **39**, 101 (2001)
123. J.H.Kim, H.-N.Cho, S.H.Kim, J.Y.Kim. *Macromolec. Res.*, **12**, 53 (2004)
124. X.M.Feng, X.P.Ai, H.X.Yang. *Electrochem. Commun.*, **6**, 1021 (2004)
125. H.Zhong, C.Kong, H.Zhan, C.Zhan, Y.Zhou. *J. Power Sources*, **216**, 273 (2012)
126. L.Xia, L.M.Zhu, H.Y.Zhang, X.P.Ai. *Chin. Sci. Bull.*, **57**, 4205 (2012)
127. J.Li, J.Chen, H.Lu, M.Jia, L.Jiang, Y.Lai, Z.Zhang. *Int. J. Electrochem. Sci.*, **8**, 5223 (2013)
128. S.Saxena, Y.Xing, D.Kwon, M.Pecht. *Int. J. Electr. Power Energy Syst.*, **107**, 438 (2019)
129. X.Zhang, S.Zheng, H.Zou, X.Zheng, Z.Liu, W.Yang, M.Yang. *Composites, Part A*, **94**, 21 (2017)
130. X.Zhang, X.Zheng, D.Ren, Z.Liu, W.Yang, M.Yang. *Mater. Lett.*, **164**, 587 (2016)
131. M.Kise, S.Yoshioka, K.Hamano, H.Kuriki, T.Nishimura, H.Urushibata. *J. Electrochem. Soc.*, **153**, A1004 (2006)
132. M.Kise, S.Yoshioka, K.Hamano, D.Takemura, T.Nishimura, H.Urushibata, H.Yoshiyasu. *J. Power Sources*, **146**, 775 (2005)
133. M.Kise, S.Yoshioka, K.Hamano, H.Kuriki, T.Nishimura, H.Urushibata, H.Yoshiyasu. *J. Electrochem. Soc.*, **152**, 1516 (2005)
134. M.Kise, S.Yoshioka, K.Hamano, H.Kuriki, T.Nishimura, H.Urushibata. *J. Electrochem. Soc.*, **153**, 1004 (2006)
135. M.Kise, S.Yoshioka, H.Kuriki. *J. Power Sources*, **174**, 861 (2007)
136. M.Baginska, B.J.Blaiszik, R.J.Merriman, N.R.Sottos, J.S.Moore, S.R.White. *Adv. Energy Mater.*, **2**, 583 (2012)
137. Y.Deng, Z.Wang, Z.Ma, J.Nan. *Energy Technol.*, **8**, 1901037 (2020)
138. R.P.Kingsborough, T.M.Swager. *J. Am. Chem. Soc.*, **121**, 8825 (1999)
139. E.V.Beletskii, Y.A.Volosatova, S.N.Eliseeva, O.V.Levin. *Russ. J. Electrochem.*, **55**, 339 (2019)
140. C.Karlsson, T.Suga, H.Nishide. *ACS Appl. Mater. Interfaces*, **9**, 10692 (2017)
141. J.Heinze, B.A.Frontana-Uribe, S.Ludwigs. *Chem. Rev.*, **110**, 4724 (2010)
142. L.F.Xiao, X.Ai, Y.L.Cao, Y.Wang, H.X.Yang. *Electrochem. Commun.*, **7**, 589 (2005)
143. S.L.Li, L.Xia, H.Y.Zhang, X.P.Ai, H.X.Yang, Y.L.Cao. *J. Power Sources*, **196**, 7021 (2011)
144. H.Zhang, Y.Cao, H.Yang, S.Lu, X.Ai. *Electrochim. Acta*, **108**, 191 (2013)
145. K.E.Thomas-Alyea, J.Newman, G.Chen, T.J.Richardson. *J. Electrochem. Soc.*, **151**, A509 (2004)
146. G.Chen, T.J.Richardson. *Electrochem. Solid State Lett.*, **7**, A23 (2004)
147. G.Chen, T.J.Richardson. *J. Electrochem. Soc.*, **157**, 735 (2010)
148. B.Wang, T.J.Richardson, G.Chen. *Phys. Chem. Chem. Phys.*, **15**, 6849 (2013)
149. B.Wang, T.J.Richardson, G.Chen. *J. Electrochem. Soc.*, **161**, A1039 (2014)
150. X.M.Feng, J.Y.Zheng, J.J.Zhang, R.F.Li, Z.J.Li. *Electrochim. Acta*, **54**, 4036 (2009)
151. G.Chen, T.J.Richardson. *Electrochem. Solid State Lett.*, **9**, A24 (2006)
152. J.K.Feng, X.P.Ai, Y.L.Cao, H.X.Yang. *J. Power Sources*, **161**, 545 (2006)
153. H.Zhang, Y.Cao, H.Yang, S.Lu, X.Ai. *J. Polym. Sci., Part B: Polym. Phys.*, **51**, 1487 (2013)
154. K.Zhang, W.Xiao, J.Liu, C.Yan. *J. Solid State Electrochem.*, **23**, 2853 (2019)
155. D.Ofer, R.M.Crooks, M.S.Wrighton. *J. Am. Chem. Soc.*, **112**, 7869 (1990)
156. G.Zotti, G.Schiavon. *Synth. Met.*, **39**, 183 (1990)
157. H.Mao, P.G.Pickup. *J. Am. Chem. Soc.*, **112**, 1776 (1990)
158. A.A.Fedorova, E.V.Beletskii, A.Yu.Kalnin, O.V.Levin. *J. Power Sources*, **510**, 230392 (2021)
159. R.P.Kingsborough, T.M.Swager. *Adv. Mater.*, **10**, 1100 (1998)
160. A.E.Pullen, T.M.Swager. *Macromolecules*, **34**, 812 (2001)
161. J.Hjelm, R.W.Handel, A.Hagfeldt, E.C.Constable, C.E.Housecroft, R.J.Forster. *J. Phys. Chem. B*, **107**, 10431 (2003)
162. J.Hjelm, R.W.Handel, A.Hagfeldt, E.C.Constable, C.E.Housecroft, R.J.Forster. *Inorg. Chem.*, **44**, 1073 (2005)
163. P.D.Byrne, P.Müller, T.M.Swager. *Langmuir*, **22**, 10596 (2006)
164. M.T.Nguyen, R.A.Jones, B.J.Holliday. *Macromolecules*, **50**, 872 (2017)
165. G.Salinas, B.A.Frontana-Uribe. *ChemElectroChem*, **6**, 4105 (2019)